Electronic Supplementary Information

on

Effect of metakaolin and fly ash on the early hydration and pore structure of Portland cement

Vanda Papp^{a,b}, Ioan Ardelean^c, Anna Bulátkó^d, Krisztina László^d, Attila Csík^e, Róbert Janovics^b, Mónika Kéri^{a*}

^aUniversity of Debrecen, Department of Physical Chemistry, Egyetem tér 1, Debrecen, H-4032, Hungary

^bIsotoptech Zrt., Debrecen, H-4026, Hungary

^cTechnical University of Cluj-Napoca, Department of Physics and Chemistry, 400114 Cluj-Napoca, Romania

^dBudapest University of Technology and Economics, Department of Physical Chemistry and Materials Science, H-1521, Budapest, PO Box 91, Hungary

^eInstitute for Nuclear Research, H-4026, Debrecen, Bem tér 18/C, Hungary

NMR Relaxometry

In NMR relaxometry we follow the return of the excited magnetic spins of the hydrogen nuclei (protons) in water molecules to the equilibrium state. This process can be described with relaxation time constants (T_1 or T_2). T_2 characterizes the rate of relaxation in the transverse plane. The transverse relaxation time constant depends on the mobility of the protons, thus the water types of different mobility in the sample can be distinguished. Since the intensity of the NMR peak is proportional to the water amount of the given type, the ratio of bound and more mobile water (e.g. in pores) can be determined. The observed transverse relaxation rate constant ($1/T_2$) can be expressed by the weighted average of the relaxation rate of the mobile water in the bulk-like ($1/T_{2bulk}$) and the bound water in the surface region ($1/T_{2s}$) provided fast molecular exchange between these water types:

$$\frac{1}{T_2} = \frac{V_S}{V} \frac{1}{T_{2S}} + \frac{V_{bulk}}{V} \frac{1}{T_{2bulk}} \tag{1}$$

where V is the total volume of the measurable water, V_s and V_{bulk} are the volumes of the surface water and the bulk water respectively. T_2 is the observed apparent transverse relaxation time, while T_{2bulk} and T_{2s} are the characteristic relaxation time constants of water molecules in the bulk-like and surface regions respectively.

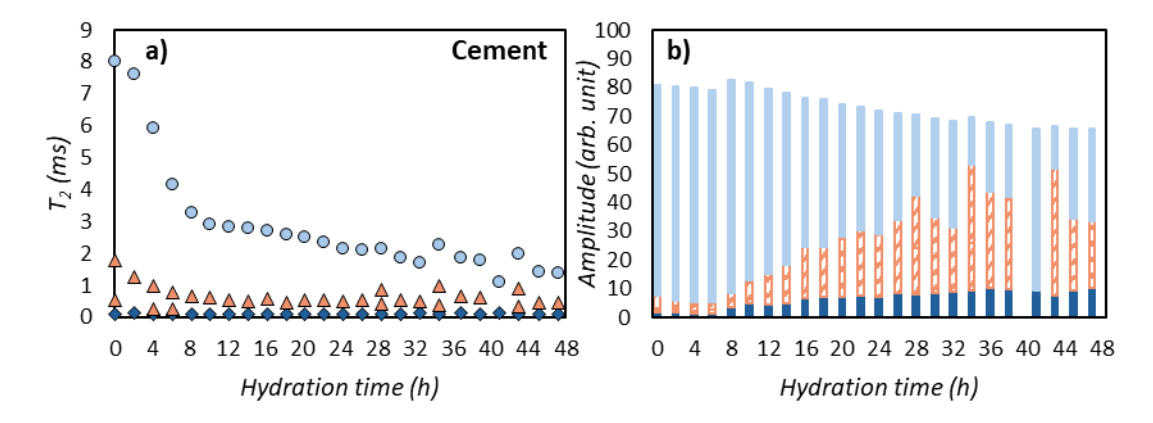


Fig. SI 1: Change of the a) T_2 relaxation time values and b) amplitudes of water types in different cement pores: intra CSH sheet (dark blue, diamond), inter CSH gel (orange, triangle) and small capillary pores (light blue, circle) over the hydration of pure Portland cement. [Papp, V., et al., State and role of water confined in cement and composites modified with metakaolin and additives. Journal of Molecular Liquids 2023, 388, 122716.]

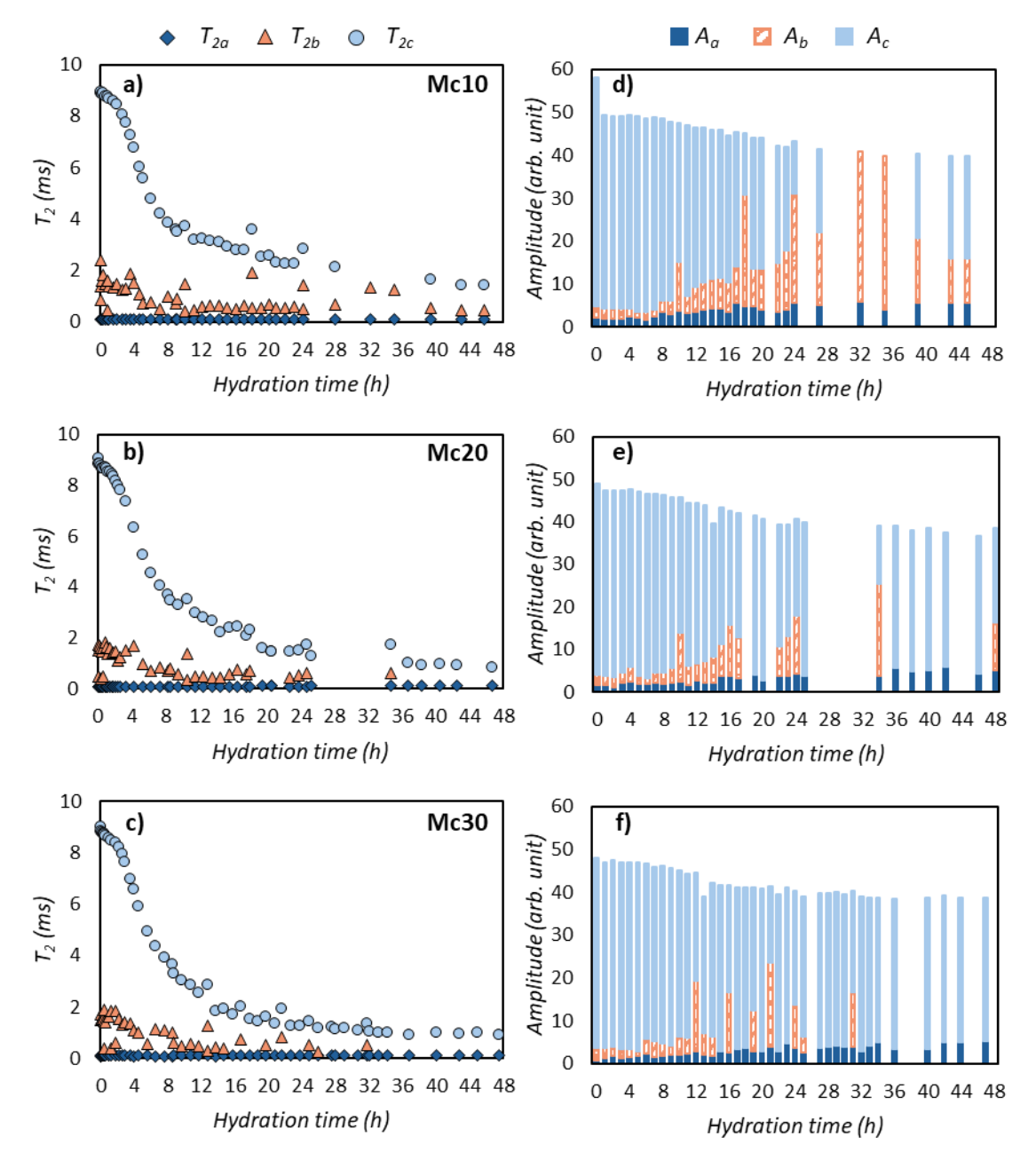


Fig. SI 2: Change of the a-c) T_2 relaxation time values and d-f) amplitudes of water types in different cement pores: intra CSH sheet (dark blue, diamond), inter CSH gel (orange, triangle) and smaller capillary pores (light blue, circle) over the hydration of 10-30% metakaolin containing cement composites.

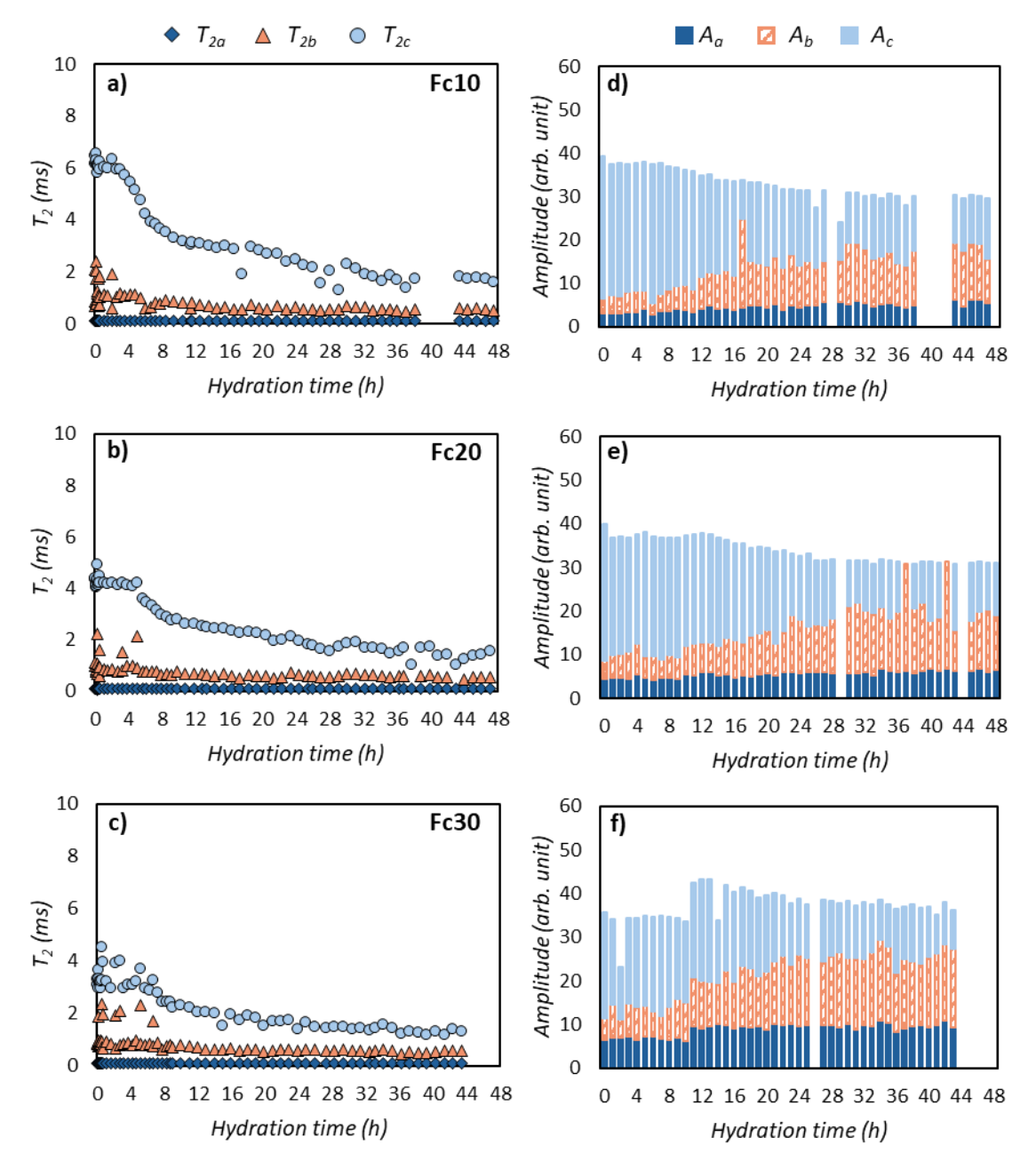


Fig. SI 3: Change of the a-c) T_2 relaxation time values and d-f) amplitudes of water types in different cement pores: intra CSH sheet (dark blue, diamond), inter CSH gel (orange, triangle) and smaller capillary pores (light blue, circle) over the hydration of 10-30% fly ash containing cement composites.

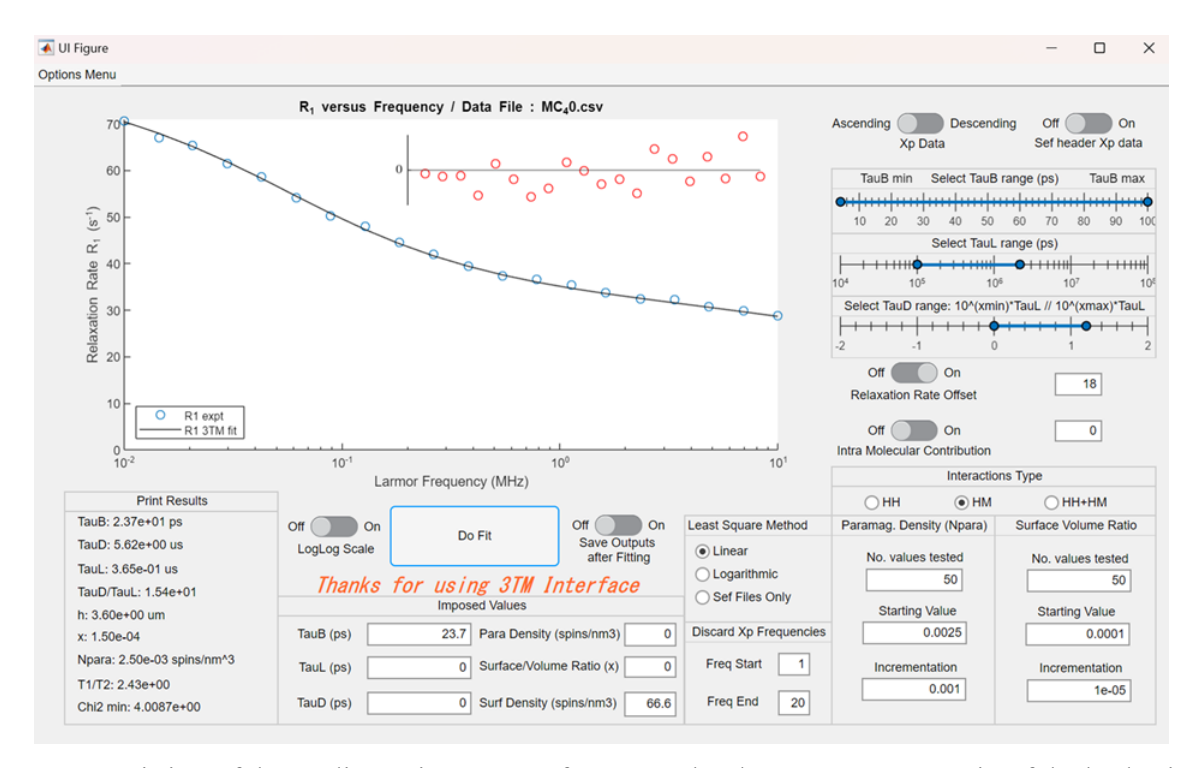


Fig. SI 4: Fitting of the T_1 dispersion curve of pure Portland cement at t= 40 min of the hydration process by 3TM fitting software provided by Kogon and Faux. The applied fitting parameters are indicated. [Kogon, R.; Faux, D., 3TM: Software for the 3-Tau Model. SoftwareX 2022, 17, 100979.]

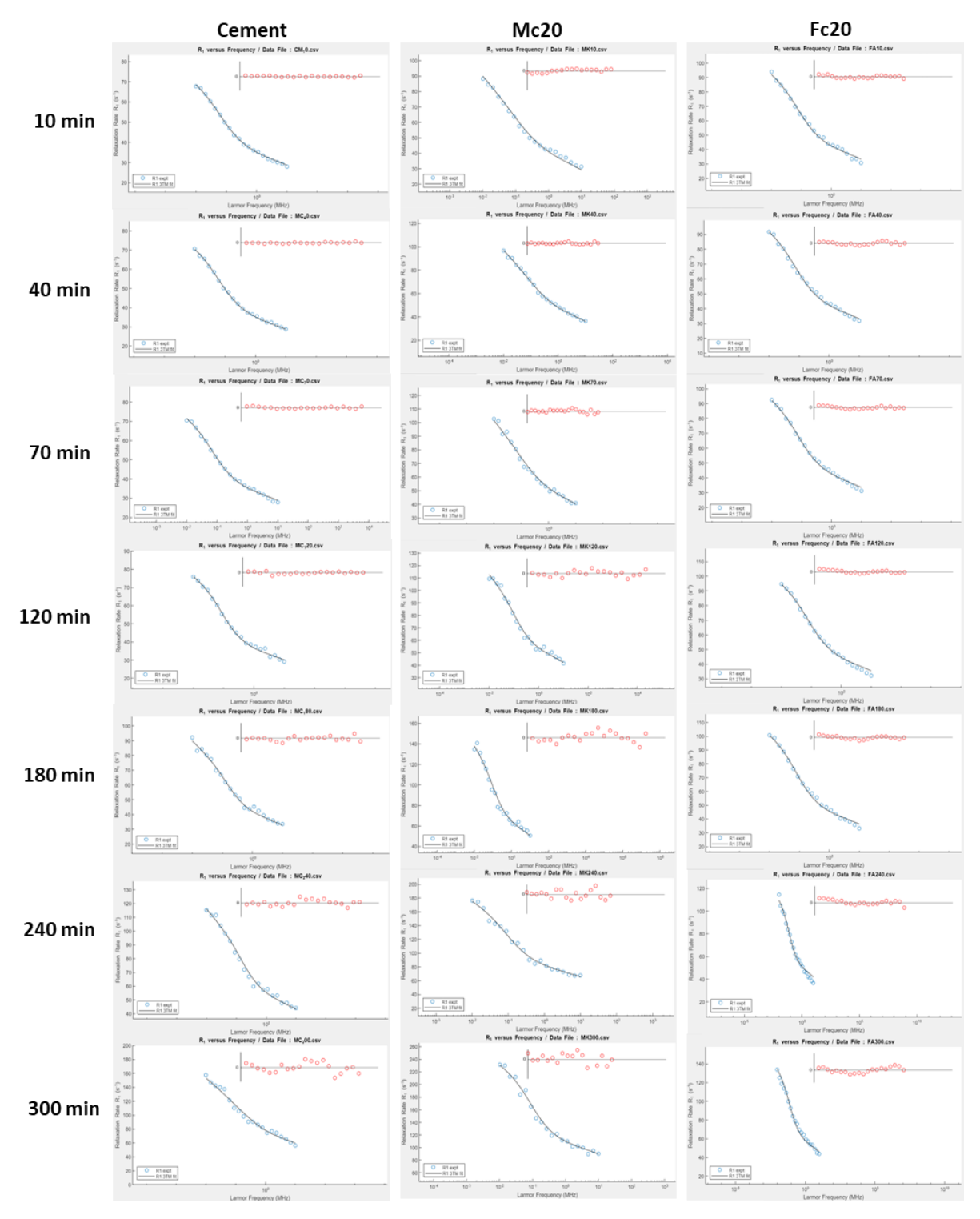


Fig. SI 5: Fittings of the T_I dispersion curves of pure Portland cement, 20% metakaolin (Mc20) and fly ash (Fc20) containing composites during the early hydration process by 3TM fitting software provided by Kogon and Faux. [Kogon, R.; Faux, D., 3TM: Software for the 3-Tau Model. SoftwareX 2022, 17, 100979.]

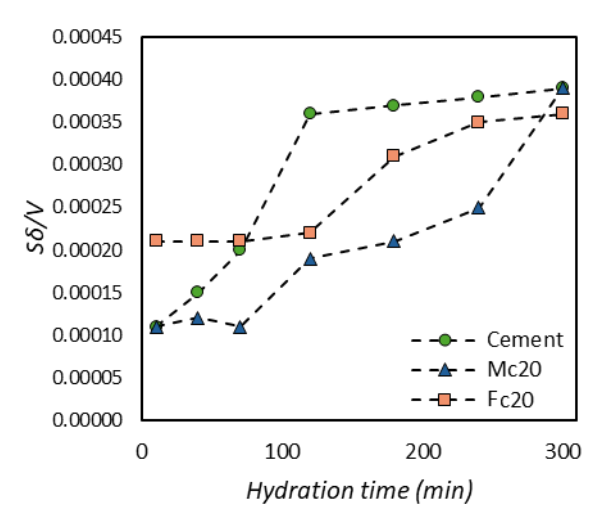


Fig. SI 6: The change of the surface layer volume to pore volume $(S\delta/V)$ during early hydration for cement, Mc20 and Fc20 samples.

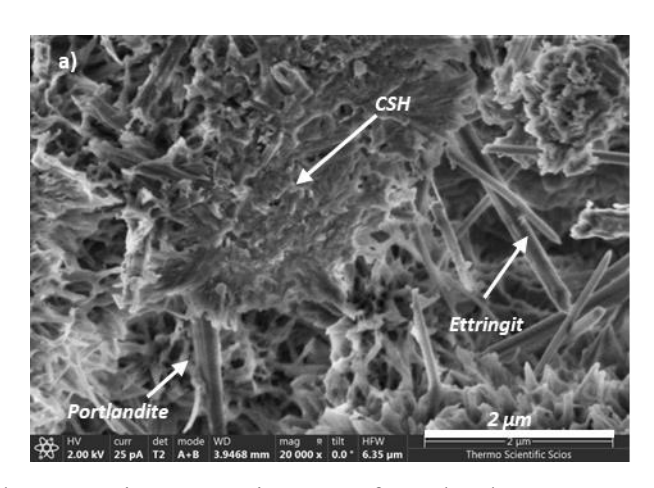


Fig. SI 7: Scanning electron microscopy images of Portland cement [*Papp, V., et al., State and role of water confined in cement and composites modified with metakaolin and additives. Journal of Molecular Liquids 2023, 388, 122716.]*

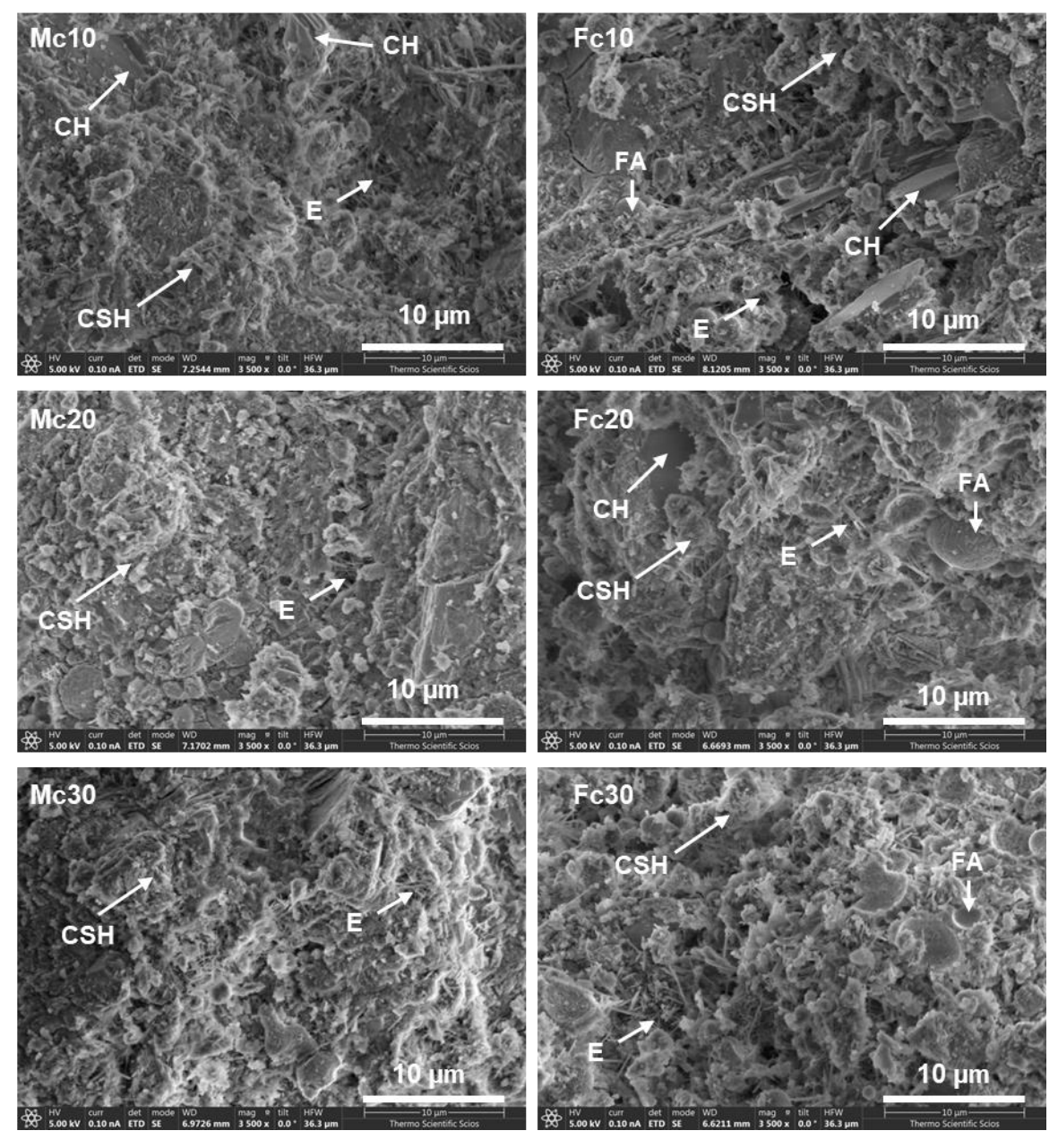


Fig. SI 8: Scanning electron microscopy images of 10-30% metakaolin (Mc10-30) and fly ash (Fc10-30) containing cement composites at a magnification of 3500. (CSH- calcium silicate hydrate, E- ettringite, CH- portlandite, FA- fly ash)

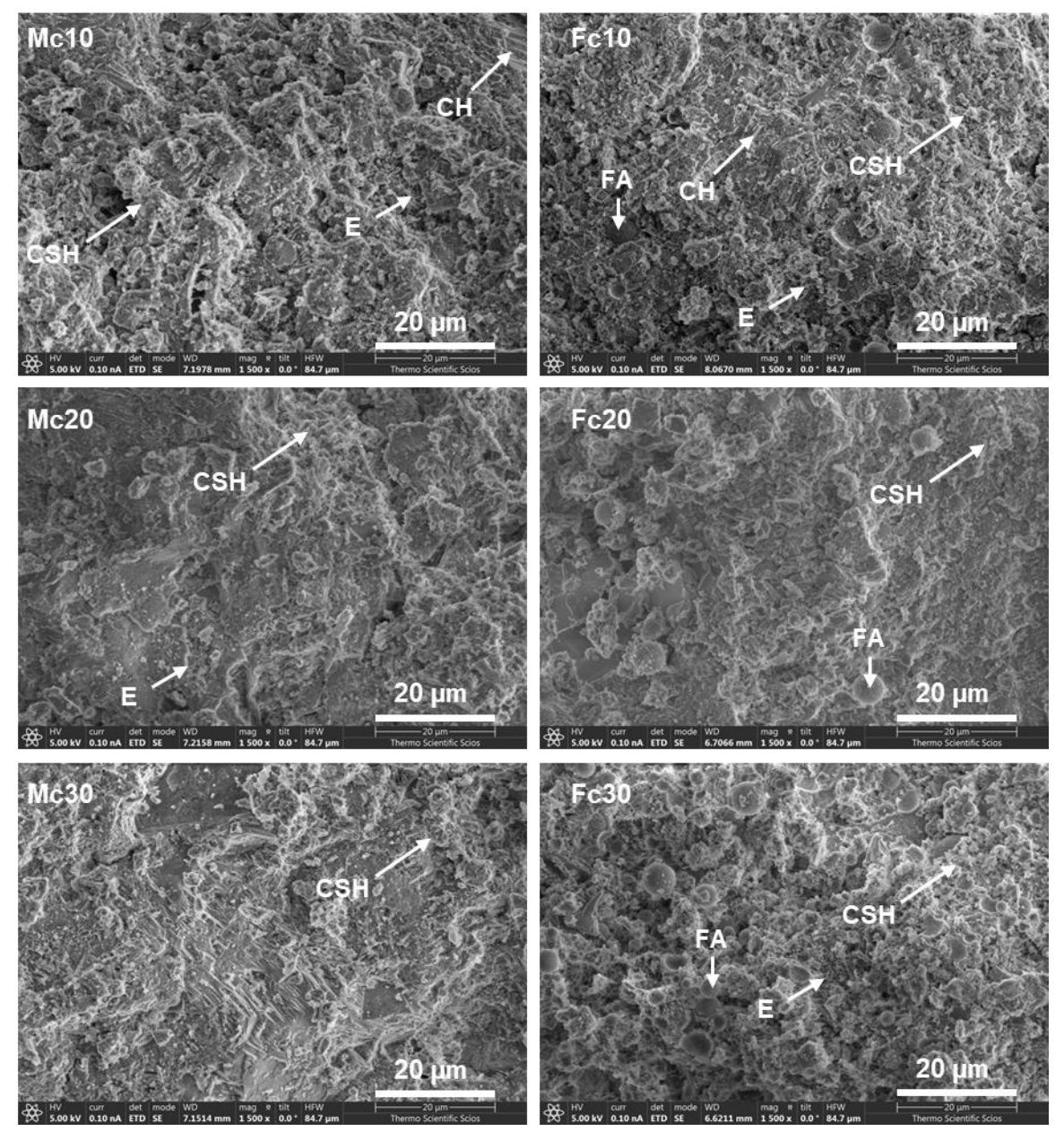


Fig. SI 9: Scanning electron microscopy images of 10-30% metakaolin (Mc10-30) and fly ash (Fc10-30) containing cement composites at a magnification of 1500. (CSH- calcium silicate hydrate, E- ettringite, CH- portlandite, FA- fly ash)

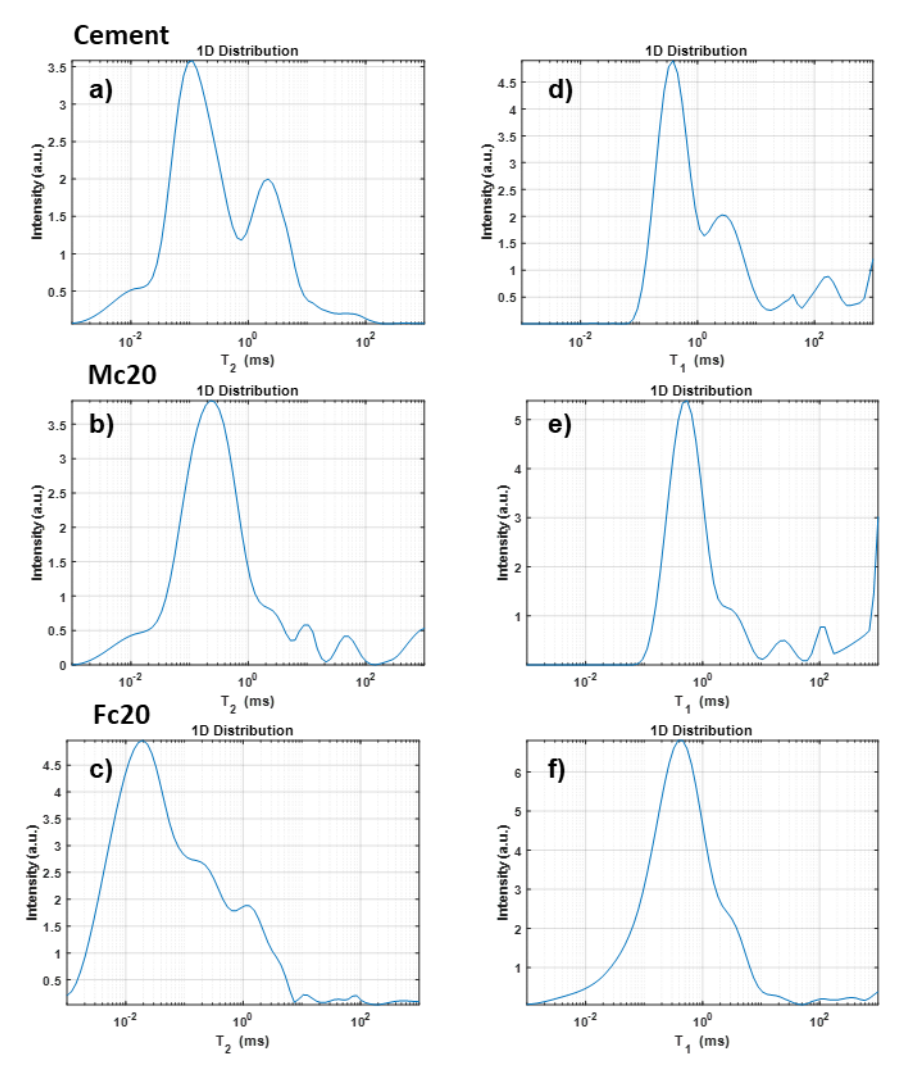


Fig. SI 10: a-c) T_1 longitudinal and d-f) T_2 transverse relaxation time distribution curves of pure Portland cement, 20% metakaolin and fly ash containing cement composites.

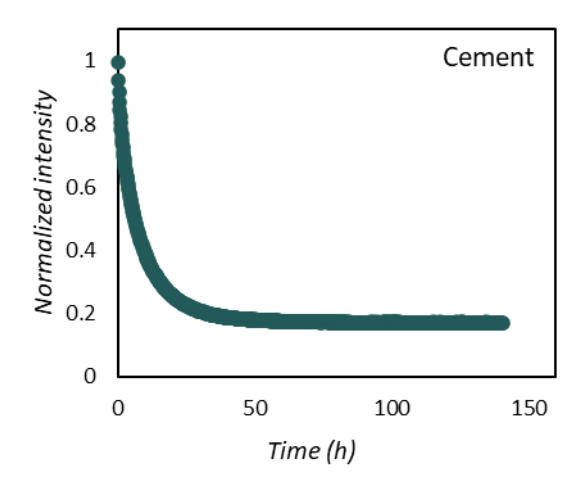


Fig. SI 11: Decay of the water signal intensity over time in pure Portland cement resulted from the H_2O - D_2O exchange diffusion measurement. [*Papp, V., et al., State and role of water confined in cement and composites modified with metakaolin and additives. Journal of Molecular Liquids 2023, 388, 122716.]*

Table SI 1: Diffusion coefficients (D_{I-3}) of confided water in 10-30% metakaolin (MC10-30) and fly ash (Fc10-30) containing cement composites.

	$D_I (\mathrm{m}^2/\mathrm{s})$	D_2 (m ² /s)	D_3 (m ² /s)
Mc10	$7.5E-11 \pm 9.3E-12$	$3.7E-11 \pm 1.8E-13$	$2.2E-12 \pm 2.7E-14$
Mc20	2.2E-11 ± 1.9E-12	$1.4E-11 \pm 4.1E-13$	$5.8E-12 \pm 2.1E-14$
Mc30	$5.0E-11 \pm 3.9E-12$	$1.0E-11 \pm 4.9E-14$	9.4E-12 ± 1.4E-12
Pc10		$1.6E-10 \pm 1.5E-12$	$5.3E-12 \pm 1.4E-13$
Pc20		$1.5E-10 \pm 2.0E-12$	$2.2E-12 \pm 2.2E-13$
Pc30		$3.7E-10 \pm 1.0E-11$	$3.8E-12 \pm 2.4E-13$